Ellipsometric study of silicon nanocrystal optical constants

Article *in* Journal of Applied Physics · April 2003

DOI: 10.1063/1.1538344 · Source: OAI

6 authors, including:

David Amans
Claude Bernard University Lyon 1
59 PUBLICATIONS **877** CITATIONS
SEE PROFILE

Ségolène Callard
Ecole Centrale de Lyon
39 PUBLICATIONS **463** CITATIONS
SEE PROFILE

J. Joseph
Ecole Centrale de Lyon
57 PUBLICATIONS **1,185** CITATIONS
SEE PROFILE

G. Ledoux
Claude Bernard University Lyon 1
142 PUBLICATIONS **3,197** CITATIONS
SEE PROFILE

Ellipsometric study of silicon nanocrystal optical constants

D. Amans,[a] S. Callard, A. Gagnaire, and J. Joseph
Ecole Centrale de Lyon, LEOM UMR CNRS 5512, 36 Avenue Guy de Collongues, F-69131 Ecully, France

G. Ledoux and F. Huisken
Max-Planck-Institut für Strömungsforschung, Bunsenstrasse 10, D-37073 Göttingen, Germany

(Received 1 February 2002; accepted 19 November 2002)

Samples of silicon nanocrystals on various substrates were prepared by cluster beam deposition of silicon nanoparticles, obtained by laser-induced pyrolysis of silane in a flow reactor. Using optical ellipsometry, the optical properties (refractive index and extinction coefficient) of the as-prepared silicon nanocrystal layers were determined in the wavelength range from 240 to 700 nm. Two dispersion models were used to describe the silicon nanocrystal optical properties: the Bruggeman effective medium approximation model and the Tauc–Lorentz model. The study showed that while a simple Bruggeman effective medium approximation model could not completely account for the silicon nanocrystal dispersion behavior, the optical response of the silicon nanocrystal layers could be satisfactorily described by a Tauc–Lorentz model. The present study also showed that, as for porous silicon, the silicon nanocrystal optical indexes significantly deviate from those of bulk crystalline and amorphous silicon. It confirms the special behavior of silicon under its nanoscale form. © *2003 American Institute of Physics.* [DOI: 10.1063/1.1538344]

I. INTRODUCTION

Porous silicon (PS) and crystalline silicon nanoparticles ($nc-\mathrm{Si}$) have become an active field of research because of their strong room temperature photoluminescence (PL).[1–5] It has been shown that naturally oxidized $nc-\mathrm{Si}$ produced by laser pyrolysis[6] has PL efficiencies that can be close to 100%.[7] Furthermore, the possibility of tuning the wavelength of the PL[6,8] makes silicon nanocrystals a very promising light-emitting material for optoelectronic devices. Recently, room-temperature voltage-tunable electroluminescence from a layer of silicon nanocrystals has been observed by Photopoulos and Nassiopoulou.[9] More recently, Pavesi *et al.*[10,11] demonstrated optical gain in $nc-\mathrm{Si}$, and Canham[12] proposed a design for a future electrically driven silicon laser. Moreover, the possibility of structuring a layer of $nc-\mathrm{Si}$ [13] may lead to devices exploiting photonic crystal structures.

For this and other applications, like microcavities or vertical cavity surface-emitting layers, it is indispensable to know the optical constants of $nc-\mathrm{Si}$, in order to calculate accurately the optical paths in the material constituting these structures.

In this article, the complex optical index N is defined as $N=n-\mathrm{i}k$ where n is the refractive index and k the extinction coefficient. A $nc-\mathrm{Si}$ layer is a stack of spherical clusters. Figure 1 shows a schematic view of a film, 35-nm-thick, composed of silicon nanocrystals with 3.5 nm diameter. These films are naturally porous and the particles are only attached on the substrates or between themselves by weak forces like electrostatic or van der Waals bondings. With the knowledge of N_{layer}, it will be possible to determine the optical properties of other $nc-\mathrm{Si}$ layers composed of the same nanoparticles, when their different degrees of porosity are taken into account. The optical constants are obtained by fitting spectroscopic ellipsometry (SE) measurements with an appropriate model. For the determination of N_{layer}, two classes of models were compared as far as their ability to fit the SE measurements are concerned: the Tauc–Lorentz (TL) model[14] and models based on the Bruggeman effective medium approximation (BEMA).[15] The validity of each model is discussed, and results are compared with previous findings on porous silicon (PS).[16–19] We also discuss the failure of the BEMA model to obtain N_{layer} since the optical indexes of the crystalline Si phase in the $nc-\mathrm{Si}$ are unknown. Finally, from a direct porosity determination, the optical constants of an assumed dense layer of $nc-\mathrm{Si}$ ($N_{nc-\mathrm{Si}}=n_{nc-\mathrm{Si}}-\mathrm{i}k_{nc-\mathrm{Si}}$), i.e., a layer without porosity, were determined.

II. EXPERIMENT AND METHOD OF ANALYSIS

Four $nc-\mathrm{Si}$ samples were prepared for the SE measurements (samples 1–4). The $nc-\mathrm{Si}$ layer used to determine N_{layer} (sample 1) was deposited on a fused silica substrate. The layer was thick enough to allow both transmission and SE measurements and to study the photoluminescence. The other three samples (2–4) were deposited on InP substrates. This material was chosen because, as a semiconductor, it has a high refractive index ensuring a good optical contrast between the layer and the substrate. Moreover, the spectral behavior of the dielectric function of InP is distinctively different from that of silicon, which again enhances the optical contrast. Sample 5, deposited on mica, was dedicated to the direct determination of the porosity. Mica is a good substrate for atomic force microscopy (AFM). All samples were synthesized at the Max-Planck-Institut für Strömungsforschung in a cluster beam apparatus that has been described in detail earlier.[6] Shortly, silicon nanocrystals are produced by pulsed CO_2 laser pyrolysis of silane in a gas flow reactor, expanded

[a]Electronic mail: damans@ulb.ac.be

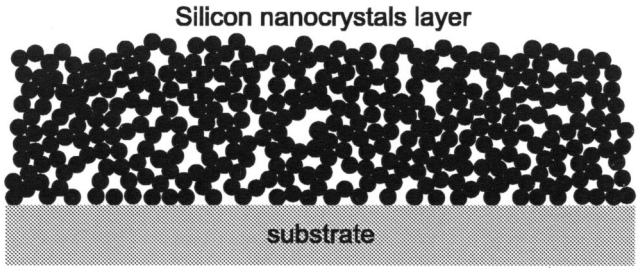

FIG. 1. Scheme of a silicon nanocrystals film. Each black circle represents one silicon nanocrystal with its surrounding oxide layer.

into a high-vacuum chamber to form a supersonic beam of nanoparticles, and finally deposited on substrates. The size distribution of the Si nanoparticles is determined *in situ* with a time of flight mass spectrometer(TOFMS). The size of the nanoparticles can be selected by means of a molecular beam chopper.[6] The deposit obtained is about 5 mm in diameter with $nc-$Si sizes ranging from 1.5 to 6 nm, from one edge to the other. The TOFMS checks the sizes of the particles deposited in the middle of the sample. The experimental conditions have been set in order to obtain a particle size of 3 nm in the middle of the sample.

The four samples used for SE measurements were studied more than three months after fabrication. Since they were kept in air this period allowed for the formation of a native oxide layer around the silicon nanocrystals and, thus, a good passivation which is necessary for a strong photoluminescence.[20]

The excellent collimation of the directed molecular beam of Si nanoparticles allows one to produce a sharp edge of the $nc-$Si film by placing a mask in front of the substrate. Such steps were fabricated on the samples 1 and 5. The layer thickness was then deduced from a topographic measurement performed by atomic force microscopy (AFM). The AFM apparatus is a multimode scanning probe microscope from Digital Instruments used in the tapping mode.

The SE experiment[21] is based on the measurement of the ratio ρ of the Fresnel reflection coefficients

$$\rho=\frac{r_p}{r_s}=\tan(\Psi)e^{i\Delta}, \tag{1}$$

where r_p and r_s are, respectively, the Fresnel reflection coefficients for a plane wave polarized parallel and perpendicular to the plane of incidence. The ellipsometric angles Δ and Ψ characterize the phase difference between the two polarizations and the amplitude ratio, respectively. A spectroscopic ellipsometer with rotating analyzer was used for the measurement. The description of the experimental setup can be found in Ref. 22. The incidence angle was 70° while the illuminated area on the sample (spot size) was $1\times3\ \mathrm{mm}^2$. Consequently, taking into account the $nc-$Si size gradient (0.9 nm/mm) present at the sample surface, the average size of $nc-$Si particles included in the spot is $3\ \mathrm{nm}\pm1.8\ \mathrm{nm}$. The spectroscopic ellipsometry measurements were carried out in the near UV and visible spectral ranges, between 240 and 700 nm in steps of 10 nm.

In case of a single layer, Ψ and Δ are entirely determined by the thickness of this layer and by the optical constants of the substrate and the layer. As the relations are nonlinear, it is necessary to use a model for fitting the SE measurements. The model considers the number of layers covering the substrate as well as their thickness and the dispersion characterizing the different materials (substrate and layers). For sample 1, a one-layer model was used. The dispersion law of fused silica (SiO_2) can be found in Ref. 23. Most of this work concerned the choice of the model for the dispersion law of $nc-$Si. Two models were tested. One model uses the Bruggeman effective medium approximation.[15] In this case, the fit parameters are the layer thickness and the volume ratios of the different materials constituting the effective medium. Another model uses the Tauc–Lorentz parametrization[14] of the optical functions. It is based on the determination of the imaginary part, ϵ_2, of the dielectric function. The energy dependence of ϵ_2 is modeled as the product of the Tauc joint density of states with a Lorentz oscillator

$$\epsilon_2(E)=\begin{cases}\dfrac{1}{E}\dfrac{AE_0C(E-E_g)^2}{(E^2-E_0^2)^2+C^2E^2} & \text{for} \quad E>E_g\\ 0 \quad \text{for} \quad E\leqslant E_g.\end{cases} \tag{2}$$

In this formula, only one oscillator is used. The parameters A, C, E_0 represent the amplitude and broadening of the oscillator and the peak transition energy, respectively. E_g is the optical band gap. The real part of the dielectric function ε_1 is obtained by Kramers–Kronig integration of ϵ_2. This integration introduces a fifth parameter, $\epsilon_1(\infty)$. Finally, since we have to introduce the layer thickness, the total number of parameters becomes 6.

The regression analysis method consists in minimizing a weighted unbiased estimator χ by varying the model parameters. The expression of χ, which measures the fit quality, is

$$\chi=\left\{\frac{1}{2M-p-1}\sum_{i=1}^{M}\left[\beta_\Psi(\delta_\Psi^i)^2+\beta_\Delta(\delta_\Delta^i)^2\right]\right\}^{1/2} \tag{3}$$

with

$$\beta_\Psi+\beta_\Delta=1, \tag{4}$$

$$\delta_\Psi^i=\tan(\Psi_{\mathrm{mes}}^i)-\tan(\Psi_{\mathrm{cal}}^i), \tag{5}$$

$$\delta_\Delta^i=\cos(\Delta_{\mathrm{mes}}^i)-\cos(\Delta_{\mathrm{cal}}^i). \tag{6}$$

The number of measured data points is M. The subscripts ''mes'' and ''cal'' designate, respectively, the measured values and the ones calculated with the theoretical model. The number of unknown model parameters are given by p. For the model using BEMA with a mixture of two materials, p is equal to 2. For the model based on the Tauc–Lorentz description of optical constants with one oscillator, p is equal to 6. The weights β_Ψ and β_Δ were introduced to take into account the different orders of magnitude of the Ψ and Δ data sets and to favor the data set having a better signal-to-noise ratio. The regression analysis method is based on the least squares solver of MATLAB 5.

The average porosity of the $nc-$Si layer was determined for sample 5. The technique consists of comparing the effective volume of the deposition, V_{dep}, with the integrated vol-

ume of the deposited silicon nanoparticles, V_{int}. To determine V_{int}, it is necessary to know both the number of silicon nanoparticles deposited per unit area and per unit time (beam intensity) and their size. To achieve this goal, we have performed a deposition with a step on a mica substrate (sample 5). This deposition lasted for 7.5 h. In order to monitor the beam intensity and the particle size distribution during the layer growth, the experiment was interrupted every 25 min for 10 s. During that time, short depositions were made on another set of mica substrates. The deposition time was kept short enough to avoid particle agglomeration on the substrate. Thus, later analysis by AFM enabled us to determine the particle beam intensity by counting the individual particles on an area of $A=6\times 6\ \mu\text{m}^2$. Furthermore, the size distribution of the Si nanoparticles was derived by measuring their height.[7] With this data as input, it was possible to determine the total number of Si particles deposited on the area A during the entire 7.5 h run, as well as their integrated volume V_{int}. On the other hand, with the height of the step measured on sample 5 (d_{dep}), the effective volume is $V_{\text{dep}}=Ad_{\text{dep}}$. As a result, the porosity, f, of the thick layer is given by $f=(V_{\text{dep}}-V_{\text{int}})/V_{\text{dep}}=1-V_{\text{int}}/V_{\text{dep}}$.

For sample 1, we also investigated the photoluminescence (PL) of the Si nanocrystals. The setup consisted of a mercury arc lamp (100 W dc) as the light source. The excitation wavelength extending from 320 to 380 nm was selected by using a bandpass filter and a blue filter to remove the second order of the bandpass filter. The detection system was composed of an optical fiber to transmit the PL light, a high wavelength pass filter (400 nm), and a charge coupled device camera. The spectra were measured from 450 to 822 nm. Finally, the spectra were corrected for the wavelength dependence of the optical response of the detection system. The transmission spectrum of sample 1 was measured with a Perkin-Elmer lambda 45 UV/Vis spectrometer.

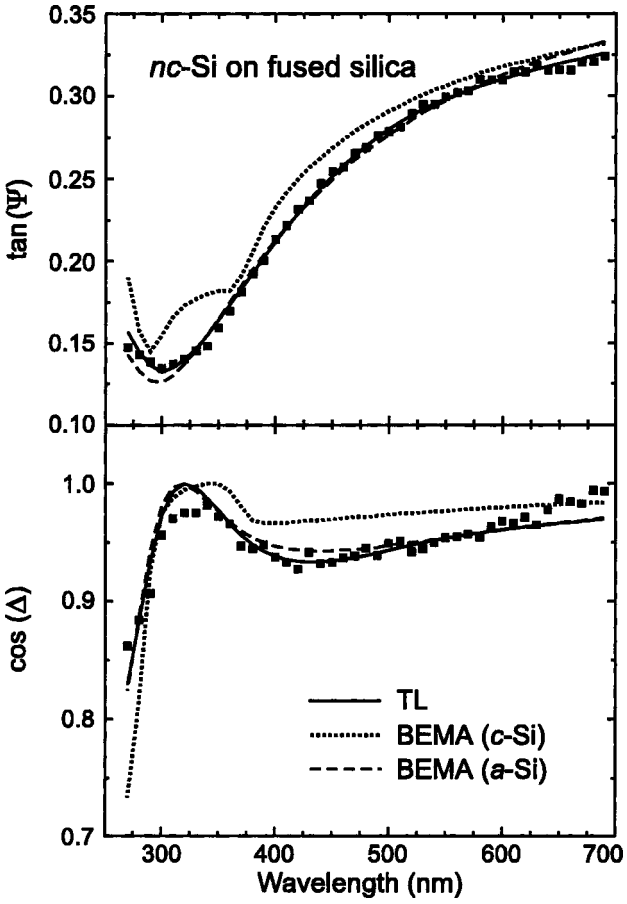

FIG. 2. Measured and calculated ellipsometric spectra for the $nc-$Si layer deposited on fused silica. The squared data points represent the measured values. The solid curve results from fit 1 (Table I) obtained by modeling the optical constants with a Tauc–Lorentz model. The dashed line corresponds to a BEMA mix of *a*-Si and SiO_2 (fit 2 in Table I) while the dotted curve results from a BEMA mix of *c*-Si and SiO_2 (fit 3 in Table I).

III. RESULTS

The spectroscopic ellipsometry measurements carried out on sample 1 are shown in Fig. 2 by the squared data points. In the same figure, we have also included the best fits obtained with the different models discussed in the previous section. The fit results as well as the χ values are reported in Table I. The minimization was performed in the spectral range from 270 to 690 nm. The weights β_Ψ and β_Δ [see Eq. (3)] were taken to be 0.9 and 0.1, respectively. The figure shows a comparison of the best results obtained with the Tauc–Lorentz and BEMA models. For the BEMA model calculations, we assumed a mixture of SiO_2 (Ref. 23, page 760) and either crystalline silicon (*c*-Si)[24] or amorphous silicon (*a*-Si).[25] It is seen that the solid line representing the Tauc–Lorentz fit gives the best agreement with the experiment.

In Fig. 3, we have plotted the optical constants n_{layer} and k_{layer} of $nc-$Si sample 1 derived from the Tauc–Lorentz fit. The best-fit parameters are $A=26.671$, $C=6.036$, $E_0=6.508$ eV, $E_g=2.315$ eV, $\epsilon_1(\infty)=2.004$, and $d=35.8$ nm. The layer thickness, d, deduced from the fit compares very favorably with the value $d=33\pm 7$ nm that we determined experimentaly by measuring the height of the step on the sample with the AFM. The parameter E_g stands for the band gap. This means that the absorption starts at wavelength values below 536 nm. The spectral shape of the refractive index, n, is a bump with a maximum at 281 nm. In the wavelength range between 200 and 850 nm, n varies between 1.75 and 1.91.

The measured transmission function is shown in Fig. 4 by the dotted line. It is compared with two theoretical transmission functions. While the solid curve has been calculated from the optical constants, derived from the Tauc–Lorentz fit and presented in Fig. 3, the dashed curve is based on the BEMA model assuming a mixture of SiO_2 and *a*-Si (fit 2 in Table I). The PL spectrum of sample 1 is also included in the same figure. It will be used in the discussion part.

The data obtained from the SE measurements of the three $nc-$Si layers on InP substrate were interpreted in terms of a two layer model, assuming a layer of native InP oxide covering the InP substrate and the layer of $nc-$Si. The average thickness and the average optical constants of the native InP oxide were determined by ellipsometric measurements on an InP sample without a $nc-$Si layer. The dispersion law of InP can be found in Ref. 24. The thickness of the oxide was thus determined to be 1.59 nm. For the BEMA

TABLE I. Comparison of the different models of optical constants used to fit the SE measurements reported in Fig. 2. χ is the weighted unbiased estimator [Eq. (3)]

Fit	Model	Thickness (nm)	χ
1	Tauc–Lorentz	35.8	0.0035
2	Bruggeman 83.05% of SiO_2 in $a-Si$	27.7	0.005
3	Bruggeman 86.9% of SiO_2 in $c-Si$	43.2	0.014

model calculations we assumed a two-component mixture of In_2O_3[26] and $In(PO_3)_3$.[27] The relative contributions of the two components were then determined to be 8.4% In_2O_3 and 91.6% $In(PO_3)_3$. These values were taken to describe the oxide layers for all samples on InP substrate. To derive the optical constants of the $nc-Si$ layer, we assumed a Bruggeman mix of N_{layer} (see Fig. 3) and voids. The fit parameters for the SE measurements on samples 2–4, which are the thickness d of the $nc-Si$ layer and the percentage of voids in the BEMA mix, are listed in Table II together with the χ values. The weights β_Ψ and β_Δ [Eq. (3)] are both taken to be 0.5 for all three fits. The SE measurements carried out on samples 2 and 3 are displayed in Fig. 5 together with the best fits obtained with the BEMA model. The measured optical constants of sample 4 are not shown here because the data curve is very similar to the one of sample 2. The theoretical SE spectra for a bare InP substrate are given in Fig. 5 for comparison.

The experiment devoted to the determination of the porosity (see Sec. II) yields a value of 70.6% for a deposit with a thickness of 9 ± 1 nm (sample 5). This value can be compared with the intrinsic porosity of a dense layer of equally sized spherical particles arranged in hexagonal closest package, which is 26%. The optical constants of a hypothetical dense layer of $nc-Si$ (N_{nc-Si}) can then be calculated by using the measured porosity and the optical constants of the as-grown $nc-Si$ deposit (N_{layer}). The results are displayed in Fig. 6 by the solid curves labeled with $nc-Si$. Details of the computation and the comparison with the other curves of Fig. 6 will be discussed in the following section.

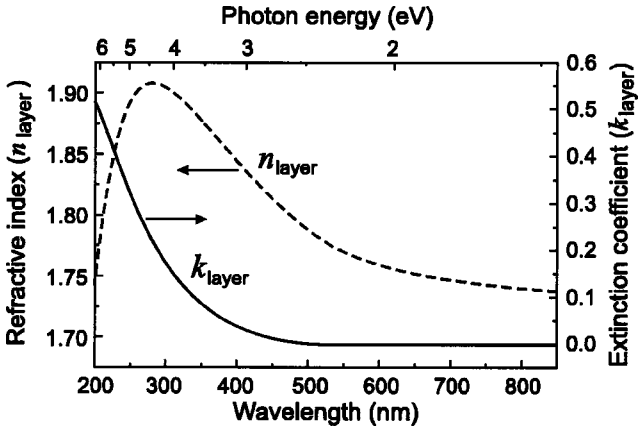

FIG. 3. This figure reports the average optical constants n_{layer} and k_{layer} of a layer of $nc-Si$ deduced from the Tauc–Lorentz (TL) model. The solid line describes the extinction coefficient while the dashed curve shows the variation of the refractive index. The parameters of the TL model are deduced from the fit of the spectroscopic ellipsometry measurements made on sample 1 (Fig. 2).

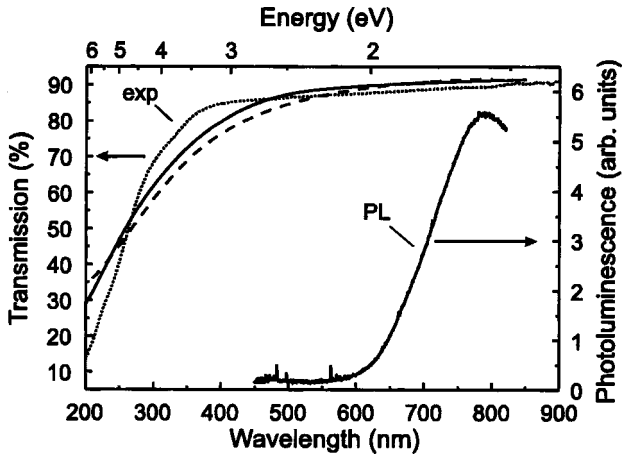

FIG. 4. The dotted curve in the upper left part of the figure reports the normalized transmission function measured on sample 1. The solid line reflects the theoretical transmission function deduced from the optical constants N_{layer} presented in Fig. 3 while the dashed curve results from a BEMA fit (fit 2 in Table I). The curve displayed in the right part of the figure represents a photoluminescence spectrum measured on the same sample.

IV. DISCUSSION

At first we will discuss the results obtained for sample 1. This was the thickest sample and, therefore, it was chosen for the determination of N_{layer}. Figure 2 and the χ values of Table I clearly show that the best fit to the ellipsometric measurement is obtained with the Tauc–Lorentz model. This fit yields a layer thickness of 35.8 nm which is very close to the value deduced from the AFM measurement (33 ± 7 nm). The TL model is particulary well suited to fit the optical constants of semiconductors in the interband region. The absorption and photoluminescence spectra presented in Fig. 4 demonstrate that the energy range studied by SE corresponds indeed to the interband region of $nc-Si$. We used the TL model with only one oscillator because the χ value did not improve when a second oscillator was included. The optical constants N_{layer} deduced from the best fit are shown in Fig. 3 in the form of the refractive index (n_{layer}) and the extinction coefficient (k_{layer}). This figure may be useful for theoretical calculation and for the design of $nc-Si$ based optical devices as microcavities.

A layer of $nc-Si$ is composed of crystalline silicon spheres, covered by their native oxide and surrounded by voids. Therefore, we have tried to describe the optical prop-

TABLE II. Fit values for the three samples on InP substrate. To model the optical constants, a BEMA mix of voids and $nc-Si$ (N_{layer}) was used. The fraction of void represents the density variation of the different samples with respect to sample 1; d is the thickness of the $nc-Si$ layer deduced from the fit. χ is the weighted unbiased estimator

Sample	Voids/No. 1 (%)	d (nm)	χ
2	19.25	12.17	0.0092
3	24.30	6.90	0.0092
4	28.82	12.37	0.013

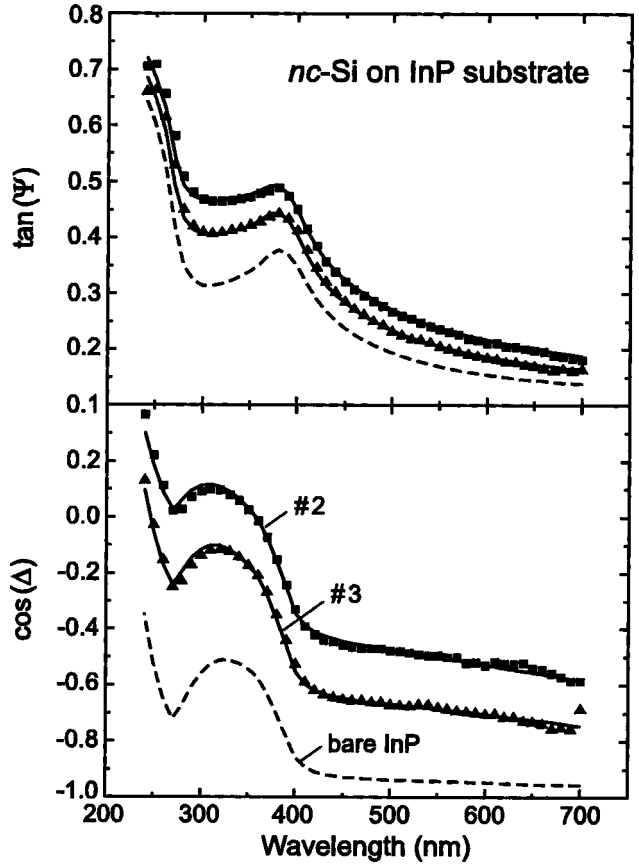

FIG. 5. Measured and calculated ellipsometric spectra for $nc-$Si layers deposited on InP. The dashed curves report the theoretical SE values for a bare InP substrate. Squares and triangles represent the experimental data obtained from samples 2 and 3, respectively (see Table II). The solid lines are the results of a BEMA fit assuming a mixture of $nc-$Si, as described by N_{layer} (Fig. 3), and voids.

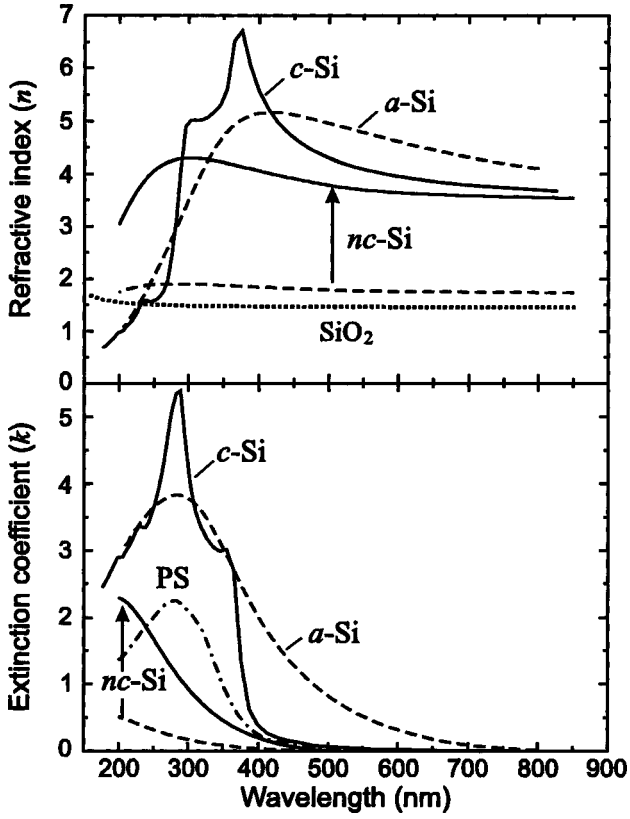

FIG. 6. Refractive index (top panel) and extinction coefficient (bottom panel) as a function of wavelength for the different materials discussed in the article. The solid and dashed curves designated by *c*-Si and *a*-Si report the optical constants of bulk crystalline[24] and amorphous[25] silicon, respectively. In the upper panel, the dotted line displays the refractive index of fused quartz (SiO_2) (see Ref. 23). In the bottom panel, the dash-dotted curve reports the extinction coefficient of porous silicon with a porosity of 79% (see Ref. 19). The lower dashed curves displayed in both panels are the result of the present work. They describe the optical constants of an as-grown layer of $nc-$Si (same curves as in Fig. 3). A hypothetical layer without voids is represented by the solid curves. The arrows connecting the latter dashed and solid curves demonstrate the effect of reducing the porosity to zero.

erties of the $nc-$Si layer of sample 1 with a BEMA mix of two or three components, as is usually done for porous silicon (PS).[5,16–18] The components, for which the optical constants are available, are SiO_2,[23] *a*-Si,[25] *c*-Si,[24] and fine grain polycrystalline silicon.[28] The fit parameters and curves of the two-component BEMA model are reported in Table I and Fig. 2, respectively. A rather bad fit is obtained for a mixture of *c*-Si and SiO_2 (fit 3). The χ value is also not reduced when voids are taken into account. This result shows that a BEMA mix containing *c*-Si is not able to reproduce the SE measurements. The failure of EMA to describe the experiment can be easily explained by the fact that the optical constants of *c*-Si show distinct structures (see Fig. 6), whereas the measured optical constants n_{layer} and k_{layer} do not reveal any fine structure besides a smooth single peak.

The Bruggeman mix of *a*-Si and SiO_2 seems to lead to an acceptable fit of the SE measurement. However, the thickness of the layer deduced from this fit is with 27.7 nm somewhat smaller than the value derived from the AFM measurement. The Tauc–Lorentz model and the Bruggeman mix of *a*-Si and SiO_2 lead to an acceptable theoretical approximation of the transmission spectrum (see Fig. 4). But both theoretical transmission curves are very close in comparison with their respective deviations from the measured spectrum. Thus, the measured transmission spectrum cannot be used to discriminate against the models. The reasonable agreement of the BEMA fit with the measured optical constants is traced back to the fact that the shape of the measured refractive index of $nc-$Si is a smooth and structureless spectral bump (see Fig. 3) while the same is true for the refractive index of *a*-Si (see Fig. 6), except that the latter is shifted to the red. On the other hand, the refractive index of the other component, SiO_2, is continuously increasing when the wavelength becomes shorter (see Fig. 6). Therefore, mixing SiO_2 and *a*-Si with an increasing contribution of SiO_2 leads to a shift of the spectral bump to higher energies and, at the same time, to a reduction of the absolute value of the refractive index. Thus, it appears that, in order to obtain a spectral bump at the right position, one has to introduce a fraction of SiO_2 which is too large. This, in turn, leads to a refractive index which is too low. The addition of voids to the BEMA mix of SiO_2 and *a*-Si does not give any improvement for the χ value. This is due to the further reduction of the refractive index when the voids are included. From this discussion it is obvious that the mixture assumed in the BEMA model can-

not represent the true fraction of the individual components in the $nc-$Si layer. This is because the $nc-$Si layer is, in fact, composed of crystalline silicon *nanoparticles* covered by an oxide and surrounded by voids. These results prove that, as shown for porous silicon,[29] the optical properties of silicon nanocrystals are quite different from those of *a*-Si and *c*-Si. Therefore, the BEMA model based on the optical index of bulk silicon cannot be physically meaningful.

We can also understand the lack of fine structure in the optical index N_{layer}. It could be the result of two effects. First, the quantum confinement in $nc-$Si causes a variation of the band structure as a function of size. This is shown, in particular, by the opening of the gap when the size of the nanocrystals drops below ~ 7 nm.[30] The opening of the gap results in a shift of the peak photoluminescence with the size, and, at the same time, the optical constants of $nc-$Si will be changed accordingly. Second, the measured optical response is the result of a convolution of the nanoparticle size distribution with the optical response of the individual Si nanocrystals. Even if the optical constants of a single $nc-$Si particle might be structured like the one of *c*-Si, the size distribution will lead to a smooth line profile. This is true, even if the size distribution is rather narrow.

We will now show that the optical index N_{layer} is also consistent with the SE measurements carried out on the three InP substrates and that this index can be used to determine the optical properties of a thin $nc-$Si deposit. The optical constants and the thickness of the samples 2–4 can be estimated by using a simple model based on a BEMA mix of voids and $nc-$Si with the latter being described by N_{layer}. In contrast to the situation with sample 1, the BEMA model should now give better results since it incorporates a proper description of the nanoparticle contribution. Indeed, even if the size distribution is not *exactly* the same from one sample to the other, Fig. 5 and Table II show that the BEMA mix of voids and silicon nanoparticles yields a good fit to the SE measurements on thin $nc-$Si deposits. The percentage of voids reflects the porosity of the sample. The good agreement displayed in Fig. 5 proves that N_{layer} is consistent with all our samples and that it can be used to calculate the optical path of a thin deposit in the frame of the BEMA model including voids.

The final goal of our study is to give an estimation of the optical constants of a hypothetical dense layer without voids that we want to describe by $N_{nc-\text{Si}}$. This complex index will represent the averaged optical constants of a given size distribution of $nc-$Si particles covered by their native oxide. In order to determine $N_{nc-\text{Si}}$, a direct measurement of the porosity was performed. The deposits of $nc-$Si can be considered as a stack of spheres with a Gaussian size distribution. But for a thin deposit containing only a few monolayers, the porosity can be strongly affected by the surface roughness. The porosity increases with decreasing layer thickness. Thus, for a very thin layer, a porosity is not defined since it is only a characteristic quantity for the volume. The thickness of the layer used for the porosity determination (sample 5) is 9 nm. Given the size variation on the samples studied, this thickness corresponds to 3–6 $nc-$Si monolayers. To deduce from the direct measurement of the porosity the optical constants of a dense layer of $nc-\text{Si}$ ($N_{nc-\text{Si}}$), it is necessary to have a direct measurement of the optical constants of a 9-nm-thick layer ($N_{d=9}$). This thickness is comparable with the thicknesses of the samples 2–4 (see Table II). Therefore, we chose $N_{d=9}$ to equal the averaged complex index of these three samples. $N_{nc-\text{Si}}$ is then determined in such way that the BEMA mix of $N_{nc-\text{Si}}$ with 70.6% voids (the measured porosity) yields $N_{d=9}$. However, this value of $N_{nc-\text{Si}}$ has to be taken with great care because of the various assumptions made to determine it. In particular, the measurement of the porosity is not made for the same sample as the SE measurements. Nevertheless, the computation of $N_{nc-\text{Si}}$ is very useful for comparative studies.

In Fig. 6, the results of the present study are summarized and compared with the optical constants of the materials discussed in the text. The lower dashed curves represent the optical index N_{layer}. Taking into account the porosity of the $nc-$Si layer, we obtain the black solid curves describing the optical index of a hypothetical $nc-$Si material without voids but with the same ratio of crystalline Si to SiO_x. The effect of decreasing porosity is demonstrated by the arrows. The optical constants displayed for *a*-Si,[25] *c*-Si,[24] and SiO_2[23] have been used for the BEMA model calculations. The extinction coefficient of SiO_2 is not plotted since it is close to zero in the wavelength range considered here. The extinction coefficient of a sample of PS with a porosity of 79%, represented by the dash-dotted curve, has been deduced from the absorption coefficient given by Theiß.[19]

We observe that the shapes of the optical properties *n* and *k* of nanocrystalline silicon are quite different from those of *c*-Si or *a*-Si, as it has already been observed for PS.[3] We also observe that they were different from PS itself.[3,19] The resonance is clearly shifted to shorter wavelengths (higher energies). This shift could be related to quantum confinement. Recently the same trend has been observed by Charvet *et al.*[31] on samples of silicon nanograins embedded in silica. Interestingly, the extinction curve for porous silicon does not show this effect, probably due to the presence of bigger particles and/or the influence of the silicon substrate that might bias the results. Another interesting point to be mentioned is the fact that, for large wavelengths, the real part of $N_{nc-\text{Si}}$ is very close to the refractive index of both bulk crystalline and amorphous silicon. This may be taken as an indication that $N_{nc-\text{Si}}$ is probably realistic.

V. CONCLUSION

We have shown that using a Tauc–Lorentz model was well adapted to determine the optical constants of $nc-$Si. The Bruggeman effective medium approximation (BEMA), as used in the cases of porous silicon (PS)[16–18] and polycrystalline silicon ($pc-$Si),[28] does not yield proper optical constants for $nc-$Si. Moreover, the fit parameters suffer from any physical significance. The application of the Tauc–Lorentz model yields the averaged optical constants of a layer of $nc-$Si including voids denoted by N_{layer}. This complex index can be used to determine the optical path in thin $nc-$Si deposits by performing SE measurements and applying the simple BEMA model.

The shape of the optical index N_{layer} is definitely different from the shape of the optical constants of *c*-Si. Moreover, the extinction coefficient is also different from the result of Theiß for PS.[19] For the most important part, the smooth shape of N_{layer} is probably due to the size distribution of the $nc-$Si deposit. The blueshift of the resonance must be attributed to a size effect which has its origin in the quantum confinement. This study completes the results already obtained from PL measurements[7,32] showing that the gap energy increases as the size of $nc-$Si decreases. From the present results, it can be concluded that $nc-$Si has an electronic band structure quite different from that of bulk silicon.

ACKNOWLEDGMENTS

D.A. thanks La Region Rhone-Alpes for financial support. G.L. is grateful to the Alexander von Humboldt foundation for a fellowship.

[1] L. T. Canham, Appl. Phys. Lett. **57**, 1046 (1990).
[2] V. Lehmann and U. Gösele, Appl. Phys. Lett. **58**, 856 (1991).
[3] N. Koshida, H. Koyama, Y. Suda, Y. Yamamoto, M. Araki, T. Saito, K. Sato, N. Sata, and S. Shin, Appl. Phys. Lett. **63**, 2774 (1993).
[4] C. Pickering, M. I. J. Beale, D. J. Robbins, P. J. Pearson, and R. Greef, J. Phys. C **17**, 6535 (1984).
[5] C. Pickering, M. I. J. Beale, D. J. Robbins, P. J. Pearson, and R. Greef, Thin Solid Films **125**, 157 (1985).
[6] M. Ehbrecht and F. Huisken, Phys. Rev. B **59**, 2975 (1999).
[7] G. Ledoux, O. Guillois, D. Porterat, C. Reynaud, F. Huisken, B. Kohn, and V. Paillard, Phys. Rev. B **62**, 15942 (2000).
[8] M. A. Laguna, V. Paillard, B. Kohn, M. Ehbrecht, F. Huisken, G. Ledoux, R. Papoular, and H. Hofmeister, J. Lumin. **80**, 223 (1999).
[9] P. Photopoulos and A. G. Nassiopoulou, Appl. Phys. Lett. **77**, 1816 (2000).
[10] L. Pavesi, L. D. Negro, C. Mazzoleni, G. Franzò, and F. Priolo, Nature (London) **408**, 440 (2000).
[11] L. D. Negro, L. Pavesi, G. Pucker, G. Franzò, and F. Priolo, Opt.. Mater. **17**, 41 (2001).
[12] L. Canham, Nature (London) **408**, 411 (2000).
[13] G. Ledoux, D. Amans, J. Gong, F. Huisken, F. Cichos, and J. Martin, Mater. Sci. Eng., C **19**, 215 (2002).
[14] G. E. Jellison and F. A. Modine, Appl. Phys. Lett. **69**, 371 (1996); **69**, 2137 (1996).
[15] D. A. G. Bruggeman, Ann. Phys. (Leipzig) **24**, 636 (1935).
[16] T. Lohner, M. Fried, P. Petrik, O. Polgár, J. Gyulai, and W. Lehnert, Mater. Sci. Eng., B **69, 70**, 182 (2000).
[17] M. Fried, H. Wormeester, E. Zoethout, T. Lohner, O. Polgár, and I. Bársony, Thin Solid Films **313, 314**, 459 (1998).
[18] H. Krzyżanowska, M. Kulik, and J. Żuk, J. Lumin. **80**, 183 (1998).
[19] W. Theiß, Surf. Sci. Rep. **29**, 91 (1997).
[20] G. Ledoux, J. Gong, and F. Huisken, Appl. Phys. Lett. **79**, 4028 (2001).
[21] R. M. A. Azzam and N. M. Basharra, *Ellipsometry and Polarized Light* (North-Holland, Amsterdam, 1977).
[22] J. Joseph and A. Gagnaire, Thin Solid Films **103**, 257 (1983).
[23] E. D. Palik, *Handbook of Optical Constants of Solids* (Academic, New York, 1985).
[24] D. E. Aspnes and A. A. Studna, Phys. Rev. B **27**, 985 (1983).
[25] D. E. Aspnes, A. A. Studna, and E. Kinsborn, Phys. Rev. B **29**, 768 (1984).
[26] A. K. Muller, Phys. Status Solidi **27**, 723 (1969).
[27] Y. Robach, A. Gagnaire, J. Joseph, E. Bergignat, and G. Hollinger, Electron. Opt. **162**, 81 (1988).
[28] G. E. Jellison, M. F. Chisholm, and S. M. Gorbatkin, Appl. Phys. Lett. **62**, 3348 (1993).
[29] M. Fried, T. Lohner, O. Polgár, P. Petrik, E. Vazsonyi, L. Bársony, and J. P. Piel, Thin Solid Films **276**, 223 (1996).
[30] C. Delerue, G. Allan, and M. Lannoo, Phys. Rev. B **48**, 11024 (1993).
[31] S. Charvet, R. Madelon, and R. Rizk, Solid-State Electron. **45**, 1505 (2001).
[32] G. Ledoux, J. Gong, F. Huisken, O. Guillois, and C. Reynaud, Appl. Phys. Lett. **80**, 4834 (2002).